Original Paper

Rheological investigations in the decomposition range of the system $Na_2O-B_2O_3-SiO_2$

Markus Eberstein, Andreas Habeck and Rolf Brückner

Institut für Nichtmetallische Werkstoffe, Technische Universität, Berlin (Germany)

Three glass melts from the Vycor-type widely distributed along the mixing gap of the pseudobinary line $SiO_2-(B_2O_3:Na_2O$ = = 84:16) were investigated each one with three different thermal histories. The following rheological properties were determined by the cylinder compression method: the Newtonian and non-Newtonian flow behaviour, the stress generation modulus as a measure of the stiffness, the high-temperature tensile strength and the critical deformation rate at which the first crack appears. The influences of the fundamental glass compositions (SiO_2 content) as well as the thermal pretreatments on these properties are demonstrated and discussed on the basis of isochomal conditions (equal Newtonian viscosities). The results can be interpreted by means of the knowledge about the demixing rules and processes which lead to various rheological two-phase systems. Most drastical changes of the rheological properties are observed in the middle of the mixing gap where spinodal decomposition has its optimum and where the differentation between the matrix phase and decomposed phase is lost.

Rheologische Untersuchungen im Entmischungsbereich des Systems $Na_2O-B_2O_3-SiO_2$

Drei weit über die Mischungslücke, entlang der pseudobinären Geraden $SiO_2-(B_2O_3:Na_2O$ = 84:16), verteilte Glasschmelzen vom Vycor-Typ wurden untersucht, jede Schmelze mit drei verschiedenen thermischen Vorgeschichten. Die folgenden rheologischen Eigenschaften wurden mit der Zylinderstauchmethode bestimmt: das Newtonsche und nicht-Newtonsche Fließverhalten, der Spannungsaufbaumodul als Maß für die Steifigkeit, die Hochtemperatur-Zugfestigkeit und die kritische Deformationsgeschwindigkeit bei der Entstehung des ersten Risses. Sowohl der Einfluß der Grundglaszusammensetzung (SiO_2-Gehalt) als auch der thermischen Vorbehandlung auf diese Eigenschaften werden auf der Basis isochomer Bedingungen (gleiche Newtonsche Viskositäten) dargestellt und diskutiert. Die Ergebnisse können mit Hilfe der Kenntnis über die Entmischungsregeln und -prozesse gedeutet werden, die zu verschiedenen rheologischen Zweiphasensystemen führen. Die drastischen Änderungen in den rheologischen Eigenschaften werden in der Mitte der Mischungslücke erhalten, wo die spinodale Entmischung ihr Optimum hat und der Unterschied zwischen Matrixphase und entmischter Phase verlorengeht.

1. Introduction and objectives

Glasses of the system $Na_2O-B_2O_3-SiO_2$ are of great importance during the last decades for industry and have found a broad application as Pyrex and Vycor glasses. In these composition ranges the glass melts decompose into phases of various chemical compositions on annealing. This was the reason for numerous investigations (see for instance [1 to 6]).

Of very few interest so far have been investigations on the influence of the composition and the degree of decomposition on the rheological properties, particularly viscosity, stress generation behaviour and high-temperature strength. The intention of this article is to prepare homogeneous and decomposed glass melts with different suspended inclusions in different matrices in order to study the influence on rheological properties.

In recent investigations interesting effects have been found. Thus, in the system $PbO-B_2O_3$ with 0 to 35 mol% PbO three extreme rheological systems could be produced: one system with a low-viscous matrix and high-viscous or hard inclusions in it, one system with a high-viscous matrix and low-viscous inclusions and one system with interconnecting parts of a spinodal decomposition [7]. In each system very different properties were obtained. On the other hand, in the two-component system $Li_2O \cdot 2SiO_2$ the situation of glass-ceramic melt models was produced by partly crystallization of the melt in well-defined thermal treatments. A non-Newtonian two-step viscosity decrease and also a two-step decrease of the stiffness resistance (as a measure of the brittleness of the melts) could be found as a function of the deformation rate [8].

Therefore, it was of special scientific interest to study the rheological properties of selected sodium borosilicate glass melts with various degrees and types of decomposition. But there is also a more practical interest with respect to the workability, particularly the isochomal and isothermal workability, of the more or less decomposed borosilicate melts.

As in the investigations of [7 and 8] the rheological measurements were made by means of the cylinder compression method with a servohydraulic test machine from MTS (Material Test System) as a parallel-plate plastometer. The method is described extensively in [9]. It has three decisive advantages: first, the compressive

Received September 13, 1996.

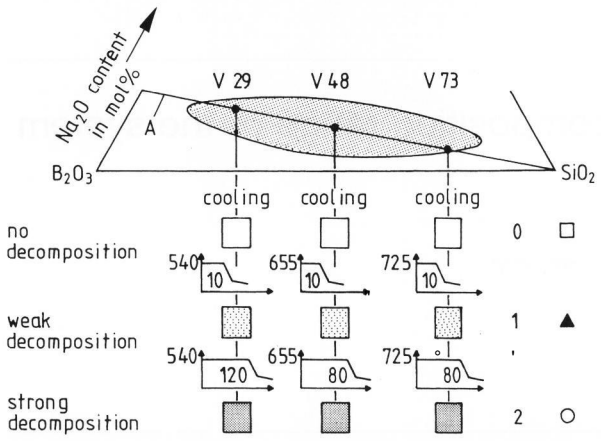

Figure 1. Survey of the investigated glass system and selection of the glass compositions inclusive thermal treatment for decomposition (semischematically). Numbers in the small diagrams are the annealing times in h and those at the ordinate are the temperatures in °C of thermal treatments of the samples.

strength is larger by one order of magnitude than the tensile strength which allows measurements within an extended stress range; second, viscoelastic properties such as stress generation modulus (stiffness), brittleness (stiffness resistance) and the high-temperature tensile strength can be obtained besides the Newtonian and non-Newtonian flow behaviour; third, most glass forming processes in industrial production are based on compressive methods at large deformation rates, thus, a practice-relevant reference is given with this method.

2. Sample selection and preparation

Compositions and heat treatments lead to very different microstructural variants of the Vycor glass system [5 and 10]. The so-called borate anomaly, which is responsible within the sodium oxide-poor range for the mixing gap, is described extensively in [4 and 5]. A formation of BO_4 tetrahedra by the presence of sodium oxide leads to a strengthening of the glass network with a maximum at $Na_2O:B_2O_3 = 16:84$ (minimum of the coefficient of thermal expansion). In the three-component system $Na_2O-B_2O_3-SiO_2$ one obtains for this ratio the so-called anomaly line A in figure 1 [5]. At the SiO_2-poor and -rich sides of this line the chemical compositions of the decomposed phases are exchanged in such a manner that also matrix and inclusions are exchanged. Therefore, fundamentally different properties of the corresponding glasses are expected.

All investigated glass melts of this study are on the A line of figure 1. The glass samples are characterized by V (Vycor glass) and by the SiO_2 content in mol%, e.g., V29 means 29 mol% SiO_2 and 71 mol% sodium borate with the ratio $Na_2O:B_2O_3 = 16:84$ (table 1). The reason for the relatively large hydroxyl content was the use of H_3BO_3 in the batch and the large solubility in B_2O_3-rich glasses. The hydroxyl content decreases with increasing SiO_2 concentration and reflects the lower amounts of borate and the smaller solubility of the hydroxyl [4].

The glass melts were heat-treated in such a way that decompositions could be obtained without, with weak and with strong turbidity. Spectroscopic measurements showed a shift of the UV absorption edge depending on the degree of decomposition (temperature and time). A minimum of transmission indicates the temperature of the maximum of decomposition. This temperature was kept constant and the shift of the points of inflexion, of the UV absorption edge was observed after various times (figures 2a and b). An asymptotic approach of the turbidity degree to a maximum value was found which served as indicator for the constitutional equilibrium of the glass system for each glass composition and temperature.

The annealing times for the strongly decomposed samples were determined by the maximum available turbidity; the glasses for which the half maximum of turbidity was obtained are the weakly decomposed samples. Table 2 shows the applied heat treatments. As expected, microstructures of the samples were obtained for the $V29_2$ sample consisting of high-viscous inclusions in a low-viscous matrix and for the $V73_2$ sample low-viscous inclusions in a high-viscous matrix [5 and 10]. While in B_2O_3-rich samples are nearly solid particles in a low viscous matrix, in the $V73_2$ sample are decomposed regions with a lower but relatively similar viscosity to the matrix viscosity. Figure 1 gives a symbolic survey about origin and heat treatment of the glasses. Index "2" means that the sample was strongly decomposed (numbers in brackets in table 2). Together with the weakly (index 1) and with the not decomposed samples (index 0) there are three different decomposition states available for each glass composition.

3. Experimental method and rheological basis

The here applied cylinder compression method is described extensively in [9]. From the stress-strain or force deformation curve (figure 3) of the compressed cylinder of a high-viscous glass melt three important properties may be obtained if two corrections are considered: the mechanical correction of the system deformation of the testing machine equipment and the thermal correction of the internal viscous heating of the sample due to the heat dissipation of the mechanical energy of compression. The first property is the stress generation modulus $E(t)_{max}$ resulting from the maximum slope of the stress-deformation curve which is a measure for the stiffness of a glass melt [11 and 12]:

$$E_{max} = (d\sigma/d\varepsilon)_{max} . \quad (1$$

This maximum value is identical with the point of inflexion of the stress-strain curve for which is valid:

$$dE_{max}/d\varepsilon = d^2\sigma/d\varepsilon^2 = 0 . \quad (2$$

The second property is the determination of the viscosity by use of the Gent equation [13] at the begin

Table 1. Composition of the glass samples V29, V48 and V73, some melting parameters and properties

	V 29	V48	V73
SiO_2 content in mol%	29	48	73
B_2O_3 content in mol%	59.64	43.68	22.68
Na_2O content in mol%	11.36	8.32	4.32
melting temperature in °C	1050	1200	1550 and 1450
melting time in h	4	4	3 and 2
T_g in °C	411	424	624
hydroxyl content in mol/l	1.43	0.95	0.34
coefficient of thermal expansion in K^{-1}	$9.84 \cdot 10^{-6}$	$8.23 \cdot 10^{-6}$	$3.33 \cdot 10^{-6}$

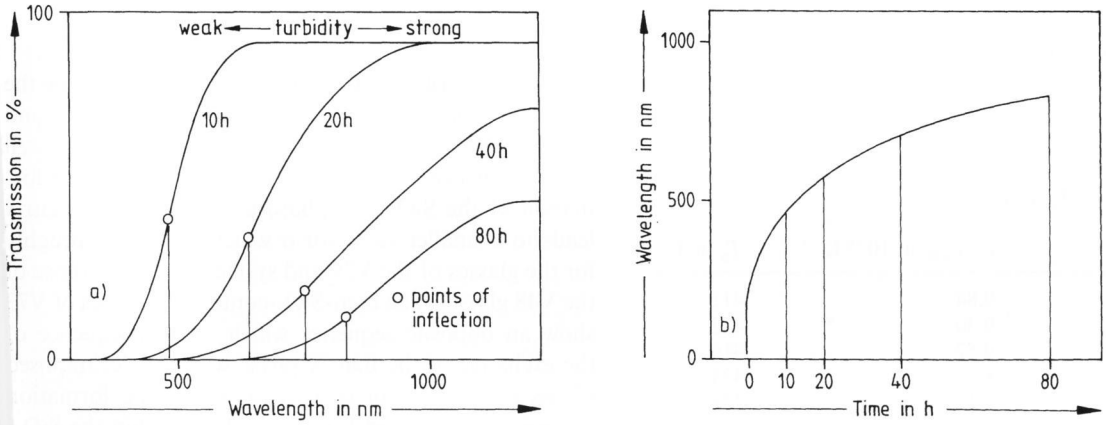

Figures 2a and b. Qualitative connection between annealing time and degree of turbidity of a Vycor glass, a) shifts of the points of inflexion of the UV absorption edges for increasing annealing times, b) wavelengths of the points of inflexion versus annealing time.

Table 2. Parameters of heat treatment and annealing to obtain the states of decomposition "weak" and "strong" based on spectrometer investigations

sample series	heat treatment at temperature in °C	states of decomposition and annealing time (in h)		
		not decomposed (0)[1)]	weakly decomposed (1)[1)]	strongly decomposed (2)[1)]
V29	540	0	10	120
V48	655	0	10	80
V73	725	0	10	80

[1)] The numbers 0, 1, 2 in brackets stand for the indices as stated in the text: 0 = not decomposed, 1 = weakly decomposed, 2 = strongly decomposed.

ing of the viscosity range, usually at a deformation of $\varepsilon = \Delta h/h_0 \approx 3\%$ where h_0 is the height of the initial cylinder and Δh its change by compression:

$$\eta(t) = F[3\,V\dot{h}(V/(2\pi h(t)^5) + 1/(h(t)^2))]^{-1} \qquad (3)$$

where V is the volume of the glass cylinder, $\dot{h} \equiv \mathrm{d}h/\mathrm{d}t$ the deformation rate and F the force. This equation is identical with the following one:

$$\eta(t) = 3m\sigma/\dot{\varepsilon} = 3(1 + R^2/(2h^2))\,\sigma/\dot{\varepsilon} \qquad (4)$$

where R is the cylinder radius, $\sigma = F/(\pi R^2)$ the axial compressive stress and $\dot{\varepsilon} = \dot{h}/h$ the deformation rate, all quantities after compression and after time t, respectively.

The third property is the maximum of the tensile stress which is situated in the equatorial line of the compressed cylindrical sample. The theoretical basis goes back to Nadai [14] and the following equation to Hessenkemper and Brückner [15]:

$$\sigma_t(t) = 3\eta(t)\dot{h}(t)[\exp(-\tfrac{3}{2}(\ln h(t) - \ln h_0) + 2\ln R_0) - R_0^2 + h(t)^2/2]/h(t)^3 \qquad (5)$$

where index 0 means the initial height and radius of the sample. This tensile stress, $\sigma_t(t)$, becomes the tensile strength, σ_{ts}, at its maximum, observable at the moment of the first crack at the equatorial line. σ_{ts} is the high-temperature tensile strength and the deformation rate at which the first crack appears is the critical deformation

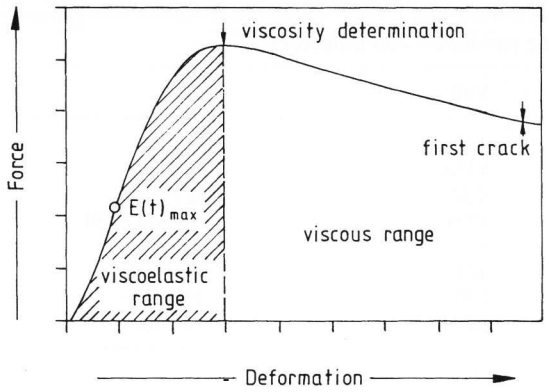

Figure 3. Typical force-deformation curve obtained from the cylinder compression method.

Table 3. Coefficients of thermal expansion, α, and transformation temperature, T_g, of all samples

sample	$\alpha_{(20/300)}$ in $10^{-6}\,K^{-1}$	T_g in °C
$V29_0$	9.84	411
$V29_1$	9.30	412
$V29_2$	9.57	416
$V48_0$	8.23	424
$V48_1$	7.17	426
$V48_2$	6.31	428
$V73_0$	3.33	624
$V73_1$	3.37	626
$V73_2$	3.63	621

rate, $\dot{h}_c$ or $\dot{\varepsilon}_c$, which depends on the amount of deformation, $\Delta h/h_0 = \varepsilon$ in such a manner that σ_{ts} increases with decreasing ε, but with increasing $\dot{\varepsilon}$ [16].

Besides these three properties which can be determined by the cylinder compression method directly and in only one experiment for one deformation, ε, and one deformation rate, $\dot{\varepsilon}$, several equations were developed [12, 17 and 18] in order to obtain the whole flow curve, i.e. the functions $\sigma = f(\dot{\varepsilon})$ and/or $\eta = f(\dot{\varepsilon})$, respectively, the Newtonian and the non-Newtonian flow behaviour. These equations were found to represent the experimental values in an optimum manner [17 and 18]. The function $\sigma(\dot{\varepsilon})$ is given by:

$$\sigma_c = m\eta_\infty \dot{\varepsilon} + \sigma_0[1 - \exp(-\dot{\varepsilon}/\dot{\varepsilon}_g)] \quad (6)$$

with

$$\sigma_0 \equiv m\dot{\varepsilon}_g(\eta_0 - \eta_\infty) \quad (7)$$

where σ_c is the thermally corrected axial compressive stress, η_0 the Newtonian viscosity at $\dot{\varepsilon} \to 0$, η_∞ the ultimate Binghamian viscosity at $\dot{\varepsilon} \to \infty$, and $\dot{\varepsilon}_g$ the flow relaxation rate. From the flow curve, equation (6), the true and apparent viscosities are obtained by the two simple operations:

$$\eta_{tru} \equiv \frac{1}{m}(d\sigma/d\dot{\varepsilon})_T \equiv \eta_\infty + \sigma_0/(m\dot{\varepsilon}_g)\exp(-\dot{\varepsilon}/\dot{\varepsilon}_g) \quad (8)$$

and

$$\eta_{app} \equiv \frac{1}{m}(\sigma/\dot{\varepsilon})_T \equiv \eta_\infty + \sigma_0/(m\dot{\varepsilon})[1 - \exp(-\dot{\varepsilon}/\dot{\varepsilon}_g)] \quad (9)$$

where m is given by equation (4) for compressive axial stress, $m = 3$ for tensile stress (elongation method) and $m = 1$ for shear stress (concentric cylinder method).

4. Results

4.1 Thermal expansion behaviour

The dilatometric investigations (tables 1 and 3) show the decrease of the coefficients of thermal expansion, α, and the increase of T_g with increasing SiO_2 content as well as the influence of the states of decomposition. The formation of the SiO_2-rich phase in the B_2O_3-rich matrix leads to a smaller value for α which is the case roughly for the glasses of the V29 and systematically for those of the V48 glasses. The high-SiO_2-containing glasses of V73 show an opposite sequence which is a consequence of the exchange of the matrix phase with the decomposed phase, an increase of α with the increasing formation of sodium borate and B_2O_3-rich phase within the SiO_2-rich matrix.

4.2 Flow behaviour

A shift of the non-Newtonian viscosity decrease toward smaller deformation rates, $\dot{\varepsilon}$, is typical for the weakly decomposed B_2O_3-rich glass melts as compared with the not decomposed clear glass melt, shown in figure 4a for example of V29. The strongly decomposed V29 glass melt, however, shows a shift back towards larger $\dot{\varepsilon}$ values up to the level of the not decomposed clear melt and even partly beyound that. The SiO_2-rich glass melt V73, show in contrast to the V29 glass melts a trend of decreasing flow relaxation rates, $\dot{\varepsilon}_g$, with increasing degree of decomposition (figure 4b).

The results of the mechanically and thermally corrected axial stresse, σ_c, correlate with the normalized apparent viscosities, η_{app}/η_0. The stresses of the weakly decomposed boron oxide-rich glass melt are lower than those of the not decomposed clear melt. Figure 5a contains the measured values of figure 4a. In contrast to that the strongly decomposed melt shows larger stress values.

The SiO_2-rich glass melt, V73, does not show remarkable alterations of the axial stresses, σ_c, with increasing degree of decomposition. Obviously the flow curves of these melts (figure 5b) are predominantly determined by the SiO_2-rich matrix even in the decomposed state by which no remarkable changes are possible. Additionally the viscosity differences between matrix and decomposed regions are smaller in these V73 glass melts than in the other glass melts, V29 and V48

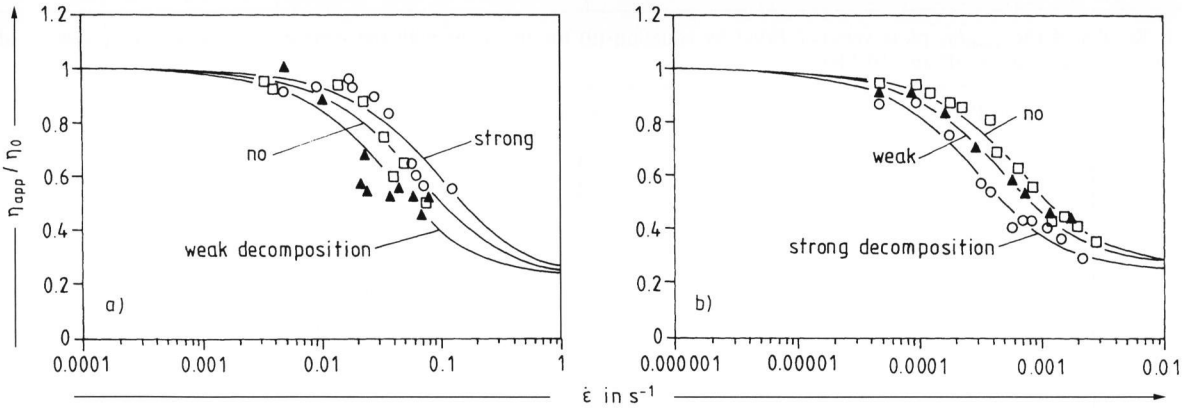

Figures 4a and b. Normalized apparent viscosity, η_{app}/η_0, versus deformation rate $\dot{\varepsilon}$ for the glass melts a) $V29_{0,1,2}$ at a Newtonian viscosity $\eta_0 \equiv 10^9$ Pa s, b) $V73_{0,1,2}$ at $\eta_0 \equiv 10^{11}$ Pa s. Solid curves fitted by equation (9). Symbols see figure 1, indices see table 2.

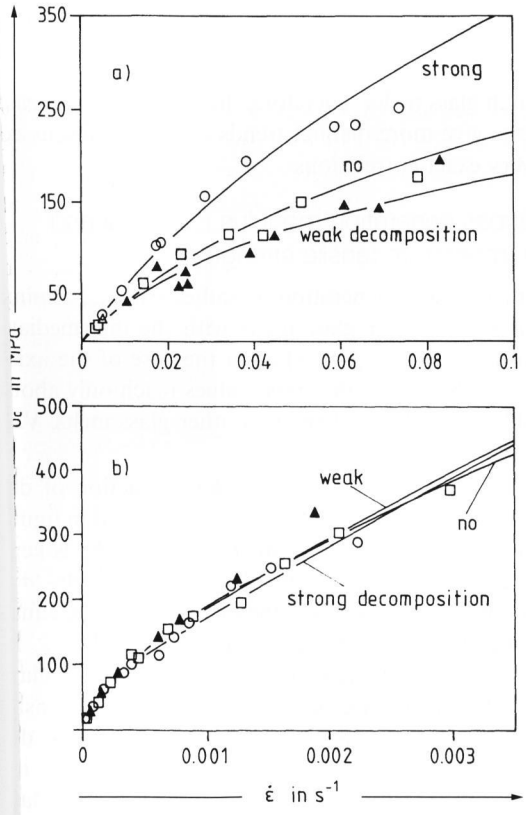

gures 5a and b. Mechanically and thermally corrected esses, σ_c, versus deformation rate, $\dot{\varepsilon}$, for the glass melts $V29_{0,1,2}$ at a Newtonian viscosity $\eta_0 = 10^9$ Pa s, b) $V73_{0,1,2}$ at $= 10^{11}$ Pa s. Solid curves fitted by equation (6). Symbols see ure 1, indices see table 2.

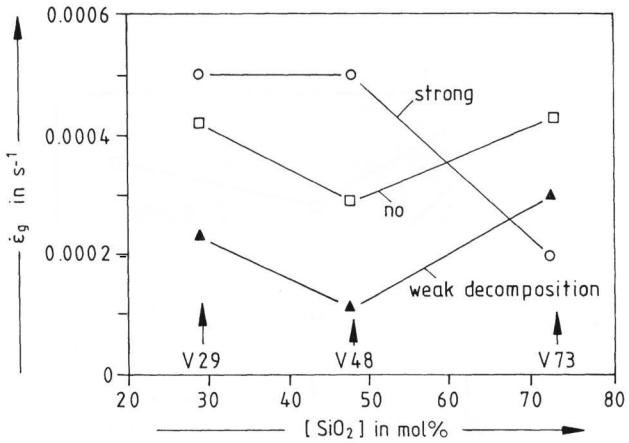

Figure 6. Flow relaxation rates, $\dot{\varepsilon}_g$, versus SiO_2 concentration of the glass melts $V29_{0,1,2}$, $V48_{0,1,2}$ and $V73_{0,1,2}$ at a Newtonian viscosity $\eta_0 \equiv 10^{11}$ Pa s.

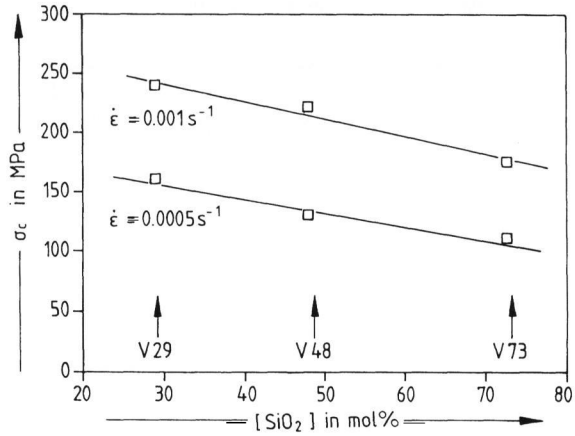

Figure 7. Corrected stresses, σ_c, versus SiO_2 concentration of the clear melts $V29_0$, $V48_0$ and $V73_0$ at $\eta_0 = 10^{11}$ Pa s and at two deformation rates, $\dot{\varepsilon}$.

A comparison of all three glass types with respect to eir flow relaxation rates, $\dot{\varepsilon}_g$, is shown in figure 6. Of ecial interest is the minimum for the not and weakly composed samples in the centre of the mixing gap, presented by melt V48. The plots of the corrected axial esses, σ_c, at equal deformation rates, $\dot{\varepsilon}$, (figure 7) show continous decrease of σ_c with increasing SiO_2 content the three glass melts. At equal quantities of defor- ation rate, less stresses are built up for samples with creasing SiO_2 content.

The results of the flow behaviour were fitted by equation (9) and the parameters of this equation are listed in table 4 together with the mean correlation coefficients, r^2, which do not fulfill in all cases mathematical and physical demands. The reason is that the corre-

Table 4. Results of the η_{app}/η_0 plots versus $\dot{\varepsilon}$ fitted by equation (9) for the melts with the various degrees od decomposition at Newtonian viscosities $\eta_0 = 10^9$ and 10^{11} Pa s

sample	η_0 in Pa s	η_∞ in Pa s	σ_0 in MPa	$\dot{\varepsilon}_g$ in s^{-1},	r^2
$V29_0$	10^9	$3 \cdot 10^8$	$1.3 \cdot 10^8$	0.0385	0.88
$V29_1$		$2.9 \cdot 10^8$	$8.4 \cdot 10^7$	0.0236	0.70
$V29_2$		$3.9 \cdot 10^8$	$2.8 \cdot 10^8$	0.06	0.86
$V48_0$		$2.8 \cdot 10^8$	$9.6 \cdot 10^7$	0.0361	0.92
$V48_1$		$2.7 \cdot 10^8$	$7.6 \cdot 10^7$	0.027	0.87
$V48_2$		$3.2 \cdot 10^8$	$2.2 \cdot 10^8$	0.068	0.48
$V29_0$	10^{11}	$3.4 \cdot 10^{10}$	$1.4 \cdot 10^8$	0.00042	0.83
$V29_1$		$3.7 \cdot 10^{10}$	$8.5 \cdot 10^7$	0.00023	0.76
$V29_2$		$3.5 \cdot 10^{10}$	$1.8 \cdot 10^8$	0.0005	0.78
$V48_0$		$4.4 \cdot 10^{10}$	$8.8 \cdot 10^7$	0.00029	0.83
$V48_1$		$4.9 \cdot 10^{10}$	$4.4 \cdot 10^7$	0.00010	0.90
$V48_2$		$3.8 \cdot 10^{10}$	$1.2 \cdot 10^8$	0.0005	0.46
$V73_0$		$2.7 \cdot 10^{10}$	$1.1 \cdot 10^8$	0.00043	0.98
$V73_1$		$3.1 \cdot 10^{10}$	$8.5 \cdot 10^7$	0.0003	0.97
$V73_2$		$3.2 \cdot 10^{10}$	$6.2 \cdot 10^7$	0.00019	0.97

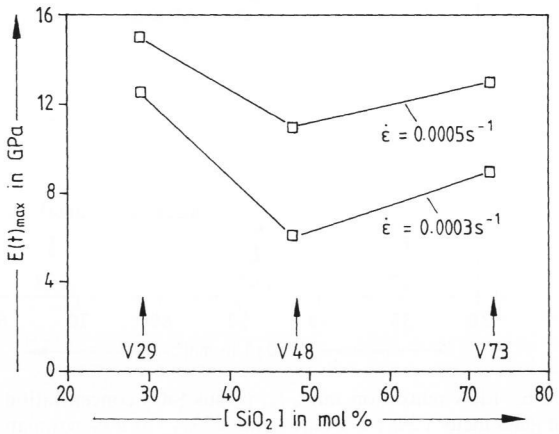

Figure 8. Stress generation modulus (stiffness), $E(t)_{max}$, versus SiO_2 concentration of the clear glass melts $V29_0$, $V48_0$ and $V73_0$ at $\eta_0 = 10^{11}$ Pa s and at two deformation rates, $\dot{\varepsilon}$.

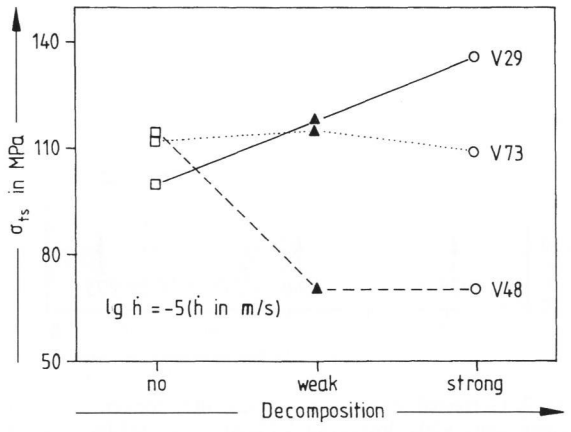

Figure 9. High-temperature tensile strength, σ_{ts}, as dependent on the degree of decomposition of the nine glass melt samples at $\eta_0 = 10^{11}$ Pa s and at $\dot{h} = 10^{-5}$ m/s.

sponding curves in the figures 4a, b and 5a, b have to be seen with respect to the large sensibility of the measurements due to the inhomogeneities especially for the B_2O_3-rich glass melts. Therefore, the results of the measurements give more distinct trends as already discussed than very exact correlations.

4.3 Stress generation modulus (stiffness) and high-temperature tensile strength

Also for the stress generation modulus, $E(t)_{max}$, a minimum is obtained for glass melts with the intermediat composition, V48, (figure 8) as in the case of the axia stresses, σ_c. Similarily the stress values reach only abou the half of the values of the two other glass melts, V2 and V73.

A very different behaviour under the action of de composition of the three glass melts is observed in figu 9 in which the deformation rate, $\dot{h}$ (or $\dot{\varepsilon} = \dot{h}/h$), is ke constant in order to compare the tensile strength, σ_t the maximum tensile stress at the first crack on the equa torial line of the deformed cylindrical sample [11, 12, 1 and 16], for all nine glass melts. For the B_2O_3-rich gla melts, V29, an increase of the high-temperature tensi strength is caused by an increase of the degree of d composition. For the SiO_2-rich melts (V73) such an i crease is not observed. The not decomposed clear gla melt, $V48_0$, shows approximately equal σ_{ts} values as th clear glass melts, $V29_0$ and $V73_0$. In contrast to that th σ_{ts} values of the weakly and strongly decomposed gla melts $V48_{1,2}$ show very small values of the order of 6 to 70 MPa. As a parallel behaviour to that is that th first cracks are observed already at small deformatic rates, $\dot{h}$, but large deformation degrees, $\Delta h/h_0$, of the samples. This is shown by a comparison of the critic deformation rates, $\dot{h}_c$, at the moment of the appearan of the first crack (figure 10).

In principle, a decrease of the high-temperature te sile strength is obtained with increasing degree of d composition for all three glass melts, however, the large decrease is observed for glass melt V48 from the cent of the mixing gap in agreement with investigations of th system $PbO-B_2O_3$ [7].

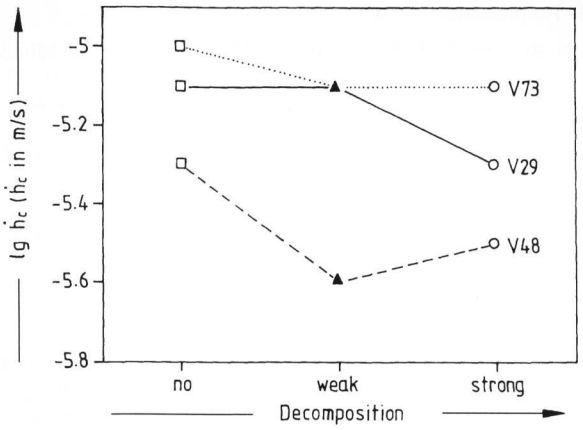

Figure 10. Critical deformation rate, $\dot{h}_c$, at which the first crack appears at large deformation degrees corresponding to the range of small deformation rates as a function of the degree of decomposition at a viscosity of $\eta_0 = 10^{11}$ Pa s.

5. Discussion

With respect to their rheological behaviour the investigated glass melts may be divided into two groups, the SiO_2-rich V73 melts on the one hand and the B_2O_3-rich V48 and V29 melts on the other hand.

The B_2O_3-rich glass melts show a distinct dependence of properties on the degree of decomposition (figures 4a and 5a). The properties of the weakly decomposed samples are shifted principally towards smaller flow relaxation rates, $\dot{\varepsilon}_g$, as compared to the clear samples. This correlates with a non-Newtonian viscosity decrease (figure 4a) at smaller deformation rates, $\dot{\varepsilon}$, and with smaller axial stresses, σ_c, (figure 5a) as well as with smaller stress generation moduli (stiffness), $E(t)_{max}$ (figure 8). If the samples are strongly decomposed, the shifts are in the opposite direction, i.e., the $\dot{\varepsilon}_g$ values increase again up to values of the clear glass melts and even beyond that. This reflects also in a shift of non-Newtonian viscosity decrease towards larger deformation rates, increasing axial stresses, and increasing stress generation moduli (stiffness). This opposite shift behaviour may be interpreted as follows. The decrease of the rheological parameters due to the weak decomposition is the consequence of the separation of SiO_2-rich particles because this amount of SiO_2 is not any more available to the structural strength of the intrinsic melt (now: the matrix) and the particles are distributed in the lower viscous matrix without mutual hindrance. On the other hand, at large degrees of decomposition the high-viscous SiO_2-rich particles are grown up to a size and/or the number of these particles is increased in such a manner that a stiffening effect of the glass melts has taken place by mutual hindrance of the SiO_2-rich particles. This is a kind of suspension effect for which the Newtonian viscosity will be increased on the one hand [8 and 19] and that of the matrix will be decreased by the reduction of the SiO_2 concentration. Both effects compete with each other and in the present case it seems that the "suspension effect" dominates a little.

The behaviour of the V73 glass melts is totally different (figures 4b and 5b). The decrease of the non-Newtonian viscosity is shifted continuously towards smaller deformation rates, $\dot{\varepsilon}$, with increasing degree of decomposition. The axial stresses, σ_c, are nearly constant and the stress generation moduli, $E(t)_{max}$, show a slight increase (figure 8). In this case, the expected formation of low-viscous B_2O_3-rich inclusions within an increasingly viscous SiO_2-rich matrix is confirmed. The SiO_2 concentration of the matrix increases indeed (and also the viscosity) but synchronously a decreasingly viscous B_2O_3-rich phase counteracts the matrix effect at least partly.

With respect to the total SiO_2 content of the three glass melts there are some peculiarities in the properties of the V48 melts within the middle of the mixing gap (figures 6 and 8). This special situation of the V48 melts has the following consequences for their rheological properties. Already the not decomposed clear glass melt, $V48_0$, has a smaller stress generation modulus (stiffness) and a smaller flow relaxation rate, $\dot{\varepsilon}_g$, than $V29_0$ and $V73_0$. On the other hand, the measured axial stresses, σ_c, (figure 7) of the three clear glass melts, $V29_0$, $V48_0$ and $V73_0$, decrease continuously along the pseudobinary line (figure 1) with increasing SiO_2 concentration at equal deformation rates, $\dot{\varepsilon}$, and equal Newtonian viscosity, η_0. This means that the generation of viscous stress decreases with increasing SiO_2 concentration, i.e., the glass melt $V73_0$ is softer or less stiff than $V29_0$.

The observed minima in $\dot{\varepsilon}_g$ and $E(t)_{max}$ (figures 6 and 8) indicate obviously a functional change of the microphases as it is the case also in other so far investigated glass systems with a mixing gap [10]. This has a destabilizing influence on the flow, on the viscoelastic behaviour and on the high-temperature tensile strength [7].

Remarkable differences are observable from the high-temperature crack behaviour of the B_2O_3-rich glass melts. The comparison of the two not decomposed melts, $V29_0$ and $V48_0$, shows approximately the same, relatively small high-temperature tensile strength, σ_{ts}. After decomposition of the samples the $V29_{1,2}$ melts tend to an increasing stability of the high-temperature fracture behaviour, while the glass melts $V48_{1,2}$ nearly break down in a manner that only up to a certain level can be spoken of a high-temperature tensile strength at all (figure 9). Additionally, the values of the critical deformation rate, $\dot{h}_c$, indicate a small ductility (figure 10). This correlates with the results on the viscosity and stiffness investigations. Obviously there is such an intensive interconnectivity of the phases that the fundamental stability of a continuous matrix is not given anymore and this points to the maximum of a spinodal decomposition in the case of V48.

In total, the results from the investigated Vycor glass system show very similar rheological properties and dependencies with respect to composition of the initial and the decomposed glass melts across the mixing gap as those from the system $PbO-B_2O_3$ [7].

6. Conclusion

The mixing gap in the system $SiO_2-B_2O_3-Na_2O$ gives rise to interesting rheological phenomena which can be interpreted with the rules of decomposition. With the cylinder compression method the influence of various two-phase systems on the flow, viscoelastic and elastic fracture properties could be studied. The obtained results and findings show the importance of the decomposition mechanisms not only for the theoretical understanding of the rheological behaviour but also for the practical workability of glass melts of the investigated three- component system.

7. List of symbols

E_{max}	stress generation modulus, as measure of stiffness of a melt (maximum value of the slope of stress-strain curve)
$F(t)$	compressive force
$h(t)$	instantaneous height of the cylindrical sample ($=h_0-\Delta h$)
h_0	initial height of the cylindrical sample
$\dot{h}$	$=\mathrm{d}h/\mathrm{d}t$ = axial deformation rate of the sample
$\dot{h}_c$	critical deformation rate of the sample at which the first crack appears for a certain deformation degree, $\Delta h/h_0$, of the sample
m	geometrical factor for shear, tension and compressive experiment, respectively
$R(t)$	instantaneous radius of the cylindrical sample
R_0	initial radius of the cylindrical sample
r	correlation coefficient
T_g	transformation temperature
t	time
V	sample volume
α	coefficient of thermal expansion
Δh	axial compressive deformation of the cylindrical sample
ε	$=\Delta h/h_0$ = axial compressive deformation degree of the sample
$\dot{\varepsilon}$	$=\mathrm{d}\varepsilon/\mathrm{d}t = \dot{h}/h$ = axial strain rate
$\dot{\varepsilon}_g$	flow relaxation rate without the influence of viscous heating
$\eta(t)$	time-dependent, thermally uncorrected viscosity
η_{app}	apparent or mean non-Newtonian viscosity
η_{tru}	true or differential non-Newtonian viscosity
η_0	Newtonian viscosity at $\dot{\varepsilon} \rightarrow 0$
η_∞	ultimate Binghamian viscosity at very large $\dot{\varepsilon}$ values
$\sigma(t)$	axial stress
σ_c	thermally corrected axial stress
σ_t	equatorial tensile stress
σ_{ts}	high-temperature tensile strength = σ_t at the first crack of the compressed glass cylinder
σ_0	fictive yield value at $\dot{\varepsilon} = 0$ of dynamic metastable Binghamian flow curve

8. References

[1] Rockett, T. J.; Foster, W. R.: The system silica–sodium tetraborate. J. Am. Ceram. Soc. **49** (1966) no. 1, p. 30–33.

[2] Hinz, W.: Silikate. Bd. 2. Die Silikatsysteme und die technischen Silikate. Berlin: VEB Verl. Bauwesen, 1971.

[3] Morey, G. W.: The ternary system $Na_2O-B_2O_3-SiO_2$. J. Soc. Glass Technol. **35** (1951) p. 270–283.

[4] Scholze, H.: Glas. 2nd ed. Berlin (et al.): Springer, 1977.

[5] Vogel, W.: Struktur und Kristallisation der Gläser. 2nd ed. Leipzig: VEB Dtsch. Verl. Grundstoffind. 1971, p. 86 ff.

[6] Haller, W.; Blackburn, D. H.; Wagstaff, F. E. et al.: Metastable immiscibility surface in the system $Na_2O-B_2O_3-SiO_2$. J. Am. Ceram. Soc. **53** (1970) no. 1, p. 34–39.

[7] Habeck, A.; Hessenkemper, H.; Brückner, R.: Influence of microheterogeneities on the mechanical properties of high-viscous melts. Glastech. Ber. **63** (1990) no. 5, p. 111–117.

[8] Deubener, J.; Brückner, R.: Influence of nucleation and crystallisation on the rheological properties of lithium disilicate melt. J. Non-Cryst. Solids **209** (1997) no. 1/2, p. 96–111.

[9] Brückner, R.; Yue, Y.; Habeck, A.: Determination of the rheological properties of high-viscous glass melts by the cylinder compression method. Glastech. Ber. Glass Sci. Technol. **67** (1994) no. 5, p. 114–129.

[10] Vogel, W.: Glaschemie. 3rd ed. Berlin (et al.): Springer, 1992.

[11] Brückner, R.; Hessenkemper, H.; Habeck, A. et al.: Stress generation modulus as a counterpart of the stress relaxation modulus. Glastech. Ber. Glass Sci. Technol. **68** (1995) no. 2, p. 70–72.

[12] Yue, Y.; Brückner, R.: Stress generation modulus and brittleness of glass melts. J. Non-Cryst. Solids **182** (1995) p. 278–285.

[13] Gent, A. N.: Theory of the parallel plate viscometer. Br. J. Appl. Phys. **11** (1960) p. 85–88.

[14] Nadai, A. L.: Theory of flow and fracture of solids. Vol. 2. New York: McGraw-Hill, 1963. p. 352–356.

[15] Hessenkemper, H.; Brückner, R.: Relaxation behaviour, high-temperature tensile strength and brittleness of glass melts. Glastech. Ber. **62** (1989) no. 12, p. 399–409.

[16] Yue, Y.; Brückner, R.: Influence of homologous substitution of chemical components on the rheological properties and on isochomal workability of silicate glass melts. Glastech. Ber. Glass Sci. Technol. **69** (1996) no. 7, p. 204–215.

[17] Brückner, R.; Yue, Y.: Non-Newtonian flow behaviour of glass melts as a consequence of viscoelasticity and anisotropic flow. J. Non-Cryst. Solids **175** (1994) p. 118–128.

[18] Yue, Y.; Brückner, R.: A new description and interpretation of the flow behaviour of glass forming melts. Non-Cryst. Solids **180** (1994) p. 66–79.

[19] Brückner, R.; Deubener, J.: Description and interpretation of the two-phase flow behaviour of melts with suspended crystals. J. Non-Cryst. Solids. (In print.)

Addresses of the authors:
M. Eberstein
Institut für Nichtmetallische Werkstoffe
Technische Universität Berlin
Englische Straße 20
D-10587 Berlin

A. Habeck
Schott Glaswerke
Hattenbergstraße 10
D-55122 Mainz

R. Brückner
Fritz-Müller-Straße 57
D-82467 Garmisch-Partenkirchen